

RESEARCH

Open Access



Optimal power allocation and throughput performance of full-duplex DF relaying networks with wireless power transfer-aware channel

Xuan-Xinh Nguyen and Dinh-Thuan Do*

Abstract

In terms of modern applications of wireless sensor networks in smart cities, relay terminals can be employed to simultaneously deliver both information and energy to a designated receiver by harvesting power via radio frequency (RF). In this paper, we propose time switching aware channel (TSAC) protocol and consider a dual-hop full-duplex (FD) relaying system, where the energy constrained relay node is powered by RF signals from the source using decode-and-forward (DF) relaying protocols. In order to evaluate system performance, we provide an analytical expression of the achievable throughput of two different communication modes, including instantaneous transmission and delay-constrained transmission. In addition, the optimal harvested power allocation policies are studied for these transmission modes. Most importantly, we propose a novel energy harvesting (EH) policy based on FD relaying which can substantially boost the system throughput compared to the conventional half-duplex (HD) relaying architecture in other transmission modes. Numerical results illustrate that our proposed protocol outperforms the conventional protocol under the optimal received power for energy harvesting at relay. Our numerical findings verify the correctness of our derivations and also prove the importance of FD transmission mode.

Keywords: Energy harvesting, Full-duplex, Decode-and-forward, Outage capacity, Delay-constrained

1 Introduction

It is undoubted that wireless communication systems have attracted much research interest in recent years. In particular, energy-aware radio access solutions can be implemented to deal with the massive increase in the consumption of energy in telecommunication networks and the efficient use of power is important for energy optimization. In addition, applications based on internet of things networks have become increasingly popular, so they require novel approaches for energy saving applied in low-power devices. Energy harvesting is the amount of energy available at the transceiver node powered by surrounding energy sources such as solar, wave, vibration, and radio frequency.

Since energy harvesting plays an important role in relaying regardless of power optimization at relays which are assumed to be powered by ideal power sources. In sensor networks and cellular networks, wireless devices using rechargeable or replaceable batteries are often out of order in a short period of time, as the battery powered devices in such wireless networks usually suffer from limited operating times. Unlike portable devices, the maintenance cost of sensor nodes is often higher in case they are replaced or recharged. Additionally, it is noted that it may be dangerous to replace batteries in toxic environments and powering medical sensors implanted inside human bodies is also challenging. To supply a perpetual power in such networks, energy harvesting is considered as a potential method to prolong lifetime of wireless devices [1, 2]. To take advantage of information transfer over wireless channels, receivers can scavenge power from the transmitted signal. Since ambient radio signals can carry energy and information, energy harvesting brings

*Correspondence: dodinhthuan@tdt.edu.vn
Wireless Communications Research Group, Faculty of Electrical and Electronics Engineering, Ton Duc Thang University, 19 Nguyen Huu Tho Street, Ho Chi Minh City, Vietnam

more major advantages compared to the conventional grid power supply [3].

Since radio frequency (RF) signals are capable of carrying both information and energy, a new concept in green wireless communications was put forward, namely simultaneous wireless information and power transfer (SWIPT). To take advantage of SWIPT, more practical receiver architectures have been developed with two separated circuits to carry out energy harvesting and information decoding [4, 5]. There are two major schemes in the receiver, including time switching and power splitting. The authors in [4] presented performance of system under capability of energy harvesting applied in a simple single-input single-output scenario while multiple-input multiple-output (MIMO) broadcasting scenarios was introduced in [6].

In order to obtain practical insights in term of optimal time and power allocation. The work in [7] focused on time allocation policy for the two transmitters in case the efficiency of energy transfer is maximized by an energy beamformer under the impact of Channel State Information (CSI) received in the uplink by the energy transmitter. Furthermore, in [8], the time fraction in TSR impacts on the optimal throughput and such parameter can be found in a numerical method.

We next consider several system models regarding existing cooperative networks with capability of energy harvesting. Firstly, the employed relay in SWIPT networks [9, 10] or the source terminal [11] can harvest energy from the radiated signal of the source terminal or the employed relay. Secondly, in multi-hop networks, energy is transferred to remote terminals via multi-hop [12, 13]. In multi-hop systems, the high path loss of the energy-bearing signal can be eliminated [12]. Unlike [12], the authors in [13] investigated a multi-antenna relay adopting two separate terminals with capability of information processing and power transfer, respectively, and the expressions of the transmission rate and outage probability were presented under the impact of remote energy transfer. In addition, relay selection is considered as solution to determine a tradeoff between the efficiency for the information transmission and the amount of energy forwarded to the energy receivers [14–16].

Furthermore, full-duplex (FD) mode was evaluated, in which it allows transmitting and receiving signals at the same frequency band at the same time slot. Various theoretical analysis and practical designs have been conducted in terms of FD networks like in [17–21]. Thanks to the use of FD mode, the resources are utilized more efficiently and it can double the spectral efficiency compared to half-duplex (HD) mode. However, due to practical constraints, the performance of FD communication can be affected by the self-interference (SI) stemming from FD node transmission.

In addition, energy harvesting along with throughput optimization has been mentioned in previous works. In [22] and [23], throughput optimization with constraints was studied under a static channel condition for obtaining best efficiency of energy harvesting transmitters.

Moreover, energy harvesting based on power control policies for wireless powered transmission over fading channels suffer from several problems, i.e., the randomness of RF energy source, wireless fading channels and the maximum power constraints. To address this situation, several existing works have considered offline optimal power control designs for fading channels [24, 25]. The work in [25] considered that the offline optimization in an efficient optimal solution was presented to achieve optimal energy efficiency. Although the authors in [26] investigated the offline scheduling and formulated the corresponding performance optimization problems of two-way relay networks, the statistics of energy and fading channels are assumed to be parameters at the transmitter, and optimal function can be derived in a numerical manner under high computation.

The authors in [27] considered that the optimal time splitting coefficients for the full-duplex dual-hop relaying lead to enhance the system throughput in comparison with the traditional half-duplex relaying scheme for all kinds of modes including instantaneous transmission, delay-constrained transmission, and delay-tolerant transmission. The energy-constrained FD relay node can be applied in the multiple-input single-output (MISO) system; the optimal power allocation and beamforming design are investigated in [28]. In another line of research, the FD decode-and-forward system using the time-switching protocol is embedded in the multiple antenna-assisted relay to obtain more energy from the source and transfer signal to the destination as in [29, 30]. Interestingly, in order to achieve the maximal throughput performance, the optimal time switching coefficient is adaptively selected based on channel state information (CSI), accumulated energy, and threshold signal-to-noise ratio (SNR) [31, 32] and [33].

Motivated from the previous works [27], we focus on optimal throughput of a two-hop case, where RF energy harvesting powers the relay. In this paper, the impact of FD transmission is investigated in terms of the system throughput to determine the performance of RF energy harvesting relaying system. The two-antenna configuration is proposed in the FD mode, where the relay is equipped with two antennas, one for transmitting signal and the other one for receiving signal simultaneously. In this paper, two different transmission modes are investigated, namely instantaneous transmission and delay-constrained transmission. Furthermore, we examine the throughput of DF relaying protocols and characterize the fundamental trade-off between energy harvesting and

system throughput. In order to compare with the effect of the FD relaying architecture, the HD relaying architecture is also investigated. The main aim of this paper is that FD relaying is an attractive and promising solution to enhance the throughput of RF energy harvesting-based relaying systems.

Comparing to [27] and [28], although this work consider a same system model with those works, our investigation also design a novel wireless power transfer strategy to improve the system performance. The authors in [27] consider a conventional time splitting protocol, in which relay switches from energy harvesting to information transfer with fixed EH fraction time allocated. While [28] design a self-energy recycling strategy for energy harvesting at relay, this EH manner can collect transmitted signal itself and scavenge to energy. Contrarily, our work redesigns the conventional time switching protocol as in [27] to a novel EH schedule. The proposed EH will acquire the channel state information (CSI) to allocate amount of EH time. In particular, the relay transmission power can be preset level. The magnitude of self interference at relay thus can be controlled based on relay transmitted power, which can improve the system performance.

The main contributions of our paper are summarized as follows:

- A new protocol for wireless power transfer called time switching aware channel protocol (TSAC) is proposed in FD DF relaying networks and further analysis is presented as well.
- We provide analytical expressions in instantaneous transmission mode for both cases, i.e., one antenna and dual antennas at relay node in EH-based networks.
- The outage probability and average throughput for delay-constrained transmission mode are derived in closed-form expressions for tractable computation. The optimal values can be achieved in various simulation results.
- The advantages of the proposed protocol are also compared with the previous works. The most critical performance metric (i.e., optimal throughput efficiency) is thoroughly analyzed and systematically validated via comparative simulations.
- It can be seen that optimal power allocation leads to enhance throughput and resulting in system performance in comparison with non-power allocation solution in the literature.

The remainder of the paper is organized as follows. In Section 2, the energy harvesting cooperative scenario with one source node equipped two antennas in FD mode is considered and two different strategies for single antenna or dual antennas for energy harvesting are

investigated. In Section 3, the power allocation in instantaneous transmission is evaluated while outage probability and optimal throughput in delay-constraint are given in Section 4 for performance evaluation. Section 5 examines HD mode for performance comparison with FD relay. Numerical results and useful insights are provided in Section 6. Eventually, Section 7 draws a conclusion for our paper.

2 System model and energy harvesting protocol

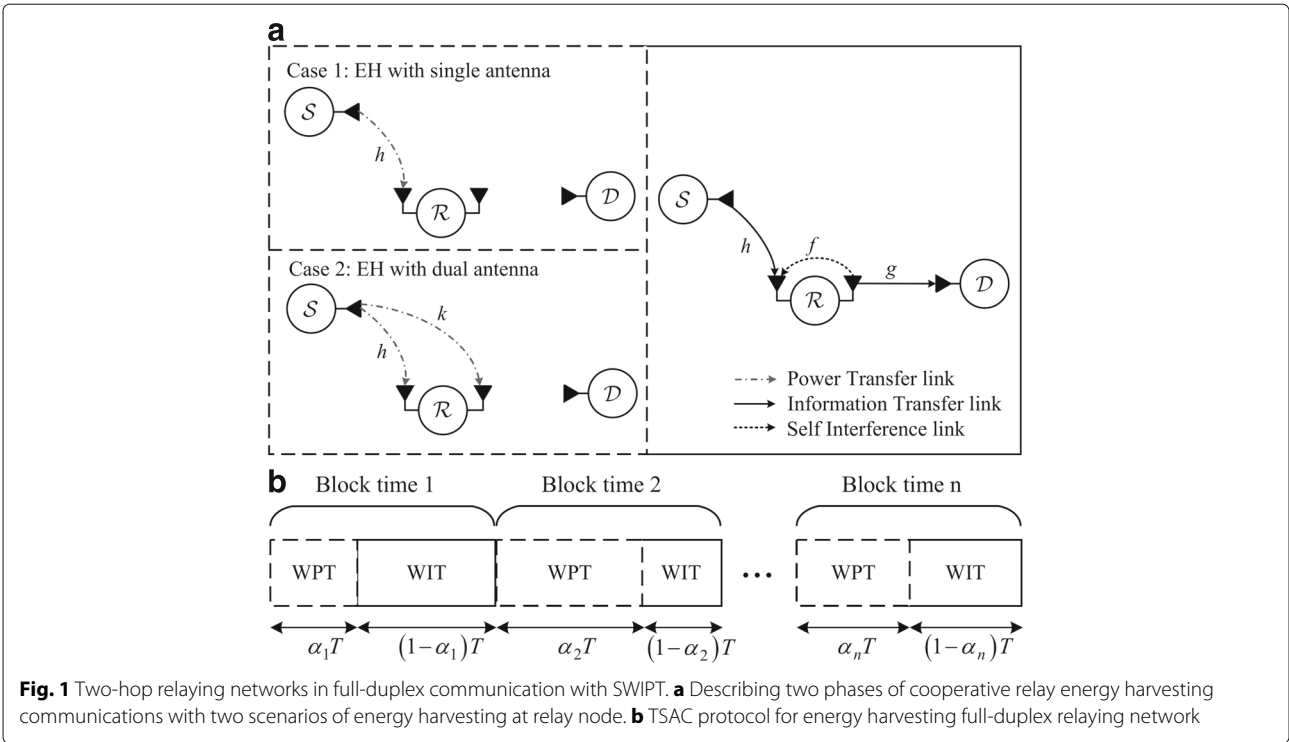
2.1 System model

As shown in Fig. 1a, we consider a two-hop relaying network consisting of one source denoted by \mathcal{S} , one destination denoted by \mathcal{D} , and one intermediate node denoted as \mathcal{R} . It is assumed that the source and destination node are equipped with single antenna, i.e., \mathcal{S} and \mathcal{D} are provided with single antenna, while \mathcal{R} is equipped with two antennas, and operated in FD mode. In addition, the relay node is assumed to have no extra embedded energy sources so it requires to harvest energy from the received RF signal from the source node [2, 5, 8, 14, 20, 27–29, 32]. The TSAC protocol is shown in Fig. 1b, in which the relay adjusts EH time to meet the installed transmit power every block time. Therefore, at time slot i th, the relay node will energy harvesting with $\alpha_i T$ seconds.

Figure 2 shows basic block diagram for the SWIPT system, where TSAC is deployed. The system has one switching unit and one combining unit compared to conventional systems as Fig. 2a or as system models introduced in [5, 27]. As illustrated in Fig. 2b, we design an architecture exploiting dual antennas to harvest energy at relay during the energy harvesting phase as [27]. In this scheme, we consider WPT phase in which the switching units change the role of both transmitting and receiving antenna to receive energy via RF signal as [27, 30]. Then, those RF signals are combined and used to feed the energy harvester. It is worth noting that case 2 is a natural choice, since it fully exploits the available hardware resources (i.e., antenna components in multiple-input multiple-output (MIMO) systems) to collect more energy [30]. Nevertheless, due to its straightforward implementation, case 1 could be more practical in certain applications.

2.2 Channel model

We assume that the $\mathcal{S} \rightarrow \mathcal{R}$ and $\mathcal{R} \rightarrow \mathcal{D}$ channel links include both large-scale path loss and statistically independent small-scale Rayleigh fading. We denote d_1 is distance between source and relay node and d_2 is distance between relay and destination node. We also denote the main channels such as h and k are the links from the source to first antenna and second antenna at relay, respectively, and g is the channel from relay to destination node. It is also assumed that the main channels experience Rayleigh fading and remain constant over the block time



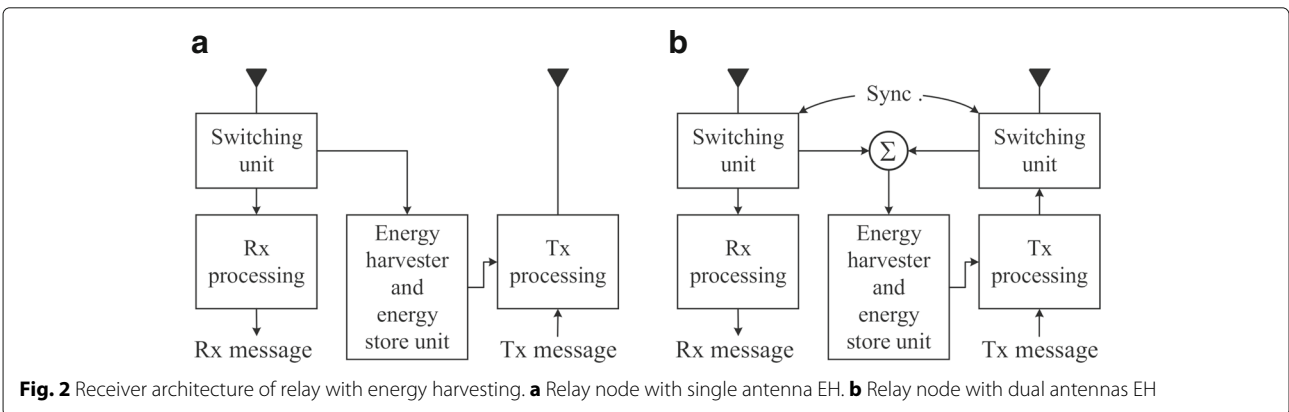
T and varies independently and identically from one block to the other.

In this paper, we also use character f to represent the SI link at relay node as normal manner. Due to the short distance of this link, the line-of-sight (LoS) path is likely to represent to SI channel; hence, it can be shown that the Rician distribution can handle such SI channel as [18]. However, due to the complicated Rician fading probability density function (PDF), the analytical expressions become extremely difficult. Fortunately, the alternative model of the Nakagami- m fading distribution provides a very good approximation to the Rician distribution. Motivated by this, and to simplify in the analysis, we adopt the Nakagami- m fading with fading severity factor m_f

and mean λ_f to model the loop interference channel in this paper.

So that $|h|^2$ and $|k|^2$ are independent and identically distributed (i.i.d.), exponential random variables with mean λ_h and λ_k , where $\lambda_h = \lambda_k$, $|g|^2$ is exponentially distributed with mean λ_g . The self-interference power link at relay, i.e., $|f|^2$, is a Gamma random variable distributed as $\Gamma(m_f, \lambda_f/m_f)$, in this paper we also assume m_f is an integer number.

The transmit power of source and relay are represented by P_S and P_R , respectively. Due to the shadowing effect, the direct transmission between source node and destination node does not exist [2, 5, 8, 20, 27, 29, 32]. The FD mode causes self-interference, which can be addressed



by the novel methods in the literature as [17, 19] and these algorithms are beyond the scope of our paper. Unfortunately, the residual self-interference still exists after interference suppression in the practical receiver architecture and it also impairs the performance of FD relay networks as [17–21, 27]. In this paper, we mainly focus on the impact of the residual self-interference on system performance in terms of the harvested power.

2.3 TSAC protocol description

In this subsection, the energy harvesting protocol is presented. In spirit of [31–33] suggesting adaptive time switching strategies for SWIPT system, we redesigned TS protocol related to CSI for FD relay transmission mode, named TSAC protocol. The detail of modified TSAC protocol is described as below. The harvested energy is stored in a rechargeable battery and then totally used to feed power circuits and transmit information to the destination node. Particularly in TSAC policy, each communication block time is slit into two slots, including wireless power transfer (WPT) slot and wireless information transfer (WIT) slot as mentioned in [4–7, 11, 12, 27, 31–33]. In each block time, WPT slot represents the first $\alpha_i T$ of block time while the WIT slot stands for the rest of $(1 - \alpha_i) T$ of block time. During WIT phase, the source transmits its symbol toward the intermediate relay simultaneously, the cooperative relay retransmits its decoded symbol to destination at the same time and bandwidth. The relay thus suffers from loop interference (LI).

Before further description, some important symbols are listed and defined in Table 1. Moreover, regarding the proposed WPT policy, \mathcal{R} will operate with the preset transmit power, $P_{\mathcal{R}}$, and thus \mathcal{R} node needs to exactly determine the time duration for WPT to harvest a sufficient amount of preset energy, $\mathcal{E}_i = P_{\mathcal{R}} (1 - \alpha_i) T$.

This process can be done as steps below. Because relay only harvests sufficient amount of energy, $\mathcal{E}_i^{EH} = f(\alpha_i)$ (where $f(\alpha_i)$ means that function of α_i), one can exactly determine the EH time by equaling amount of harvested energy and that of preset energy, i.e., $\mathcal{E}_i^{EH} = \mathcal{E}_i$. Finally, the

Table 1 List of important symbols

Symbol	Definition
P_S	The fixed transmission power, preset at source node.
$P_{\mathcal{R}}$	The fixed transmission power, preset at relay node.
\mathcal{E}_i	The relay transmission energy during time slot i th corresponding to preset power, $P_{\mathcal{R}}$.
$p_{\mathcal{R},i}^{EH}$	The harvested power from EH at relay node at time slot i th.
\mathcal{E}_i^{EH}	The relay transmission energy during time slot i th corresponding to harvested power $p_{\mathcal{R},i}^{EH}$.
α_i	The duration time allocated to EH in time slot i th.

EH time duration, α_i , is derived. It is noted that the suggested TSAC protocol does not require more additional time slot since the total frame for communication is the same as [27] (see Remark 1), and the preset relay transmit power is a constant value ($P_{\mathcal{R}}$) while the EH time is a function of the random variable WPT channel gain(s) as [31–33].

As aforementioned, to exactly determine this duration of energy harvesting time, channel gain(s) of WPT link is an important parameter(s). Therefore, we assume that the channel state information (CSI) during the first hop is available at source and relay node, which can be obtained by using novel estimation algorithm. Interestingly, the TSAC protocol adjusts the WPT time duration, α_i , in each time slot to satisfy amount of installed power $P_{\mathcal{R}}$. In contrast, the fixed-time allocation protocol in [5, 27], the harvested power, $P_{\mathcal{R}}$, vary in each block based on channel gain.

2.4 Signal model

In wireless information transfer phase (WIT) of SWIPT systems, the received signal at \mathcal{R} , $y_{\mathcal{R},i}$ and \mathcal{D} , $y_{\mathcal{D},i}$ are given respectively as follows:

$$y_{\mathcal{R},i} = \frac{h_i}{\sqrt{d_1^m}} \sqrt{P_S} x_i + f_i \sqrt{P_{\mathcal{R}}} \hat{x}_i + n_{\mathcal{R},i}, \quad (1)$$

and

$$y_{\mathcal{D},i} = \frac{g_i}{\sqrt{d_2^m}} \sqrt{P_{\mathcal{R}}} \hat{x}_i + n_{\mathcal{D},i}. \quad (2)$$

where i is the block time index, x_i and \hat{x}_i are message symbol at \mathcal{S} and decoded symbol at \mathcal{R} with unit power and zero average, respectively. We also assume that the relay decodes when $\mathcal{S} - \mathcal{R}$ link does not suffer from outage. It is assumed that $n_{\mathcal{R},i}$ and $n_{\mathcal{D},i}$ are additive white Gaussian noise (AWGN) at \mathcal{S} and \mathcal{D} in block time i th, respectively.

From (1) and (2), the signal interference noise ratio (SINR) at \mathcal{R} and \mathcal{D} in the time slot, i th are determined by

$$\gamma_i^{\mathcal{R}} = \frac{P_S |h_i|^2}{P_{\mathcal{R}} d_1^m |f_i|^2 + d_1^m \sigma_{\mathcal{R},i}^2}, \quad (3)$$

and

$$\gamma_i^{\mathcal{D}} = \frac{P_{\mathcal{R}} |g_i|^2}{d_2^m \sigma_{\mathcal{D},i}^2}, \quad (4)$$

where noise terms at \mathcal{R} and \mathcal{D} are zero mean and variances of $\sigma_{\mathcal{R},i}^2$, $\sigma_{\mathcal{D},i}^2$, respectively.

Based on the DF relaying scheme, the end-to-end SINR at block time i th, is expressed as follow

$$\gamma_i^{e2e} = \min(\gamma_i^{\mathcal{R}}, \gamma_i^{\mathcal{D}}). \quad (5)$$

In WPT time slot of SWIPT, we investigate the performance of two schemes based on the number of antennas in EH phase at relay as [27], where (i) only one antenna is

responsible for receiving signals and harvesting RF signals in EH phase or (ii) either two antennas equipped for FD communication can be used during the EH stage.

2.4.1 Single antenna for energy harvesting

In this case, only one antenna receives signals and it scavenges the RF signal to convert to DC signal. Therefore, the received signal at the relay can be expressed by

$$y_{\mathcal{R},i}^{EH} = \frac{h_i}{\sqrt{d_1^m}} \sqrt{P_S} x_i + n_{\mathcal{R},i}. \tag{6}$$

In principle, the harvested energy can be stored in an inexpensive capacitor and then entirely use for information transmission. Thus, the harvested energy at \mathcal{R} , \mathcal{E}_i^{EH} , is given by

$$\mathcal{E}_i^{EH} = \eta \alpha_i T \frac{P_S |h_i|^2}{d_1^m}, \tag{7}$$

where $0 \leq \eta \leq 1$ is the energy conversion efficiency that depends on the rectification process and the energy harvesting circuitry. It is noted that we ignore the harvested energy from noise. So that the harvested power can be determined during $(1 - \alpha_i)T$ as $P_{\mathcal{P},i}^{EH} = \mathcal{E}_i^{EH} / (1 - \alpha_i)T$.

We consider the fixed time scheme assigned for power transfer duration in [5], in which power collected at relay depends on CSI. Contrarily, in our proposed TSAC protocol, the power transmission at relay denoted by $P_{\mathcal{R}}$ corresponding with optimal throughput is preset before the transmission energy at relay thus can be calculated by

$$\mathcal{E}_i = P_{\mathcal{R}} (1 - \alpha_i) T. \tag{8}$$

Finally, in order to calculate the fraction EH time, we setting (7) equal to (8), i.e., $\mathcal{E}_i^{EH} = \mathcal{E}_i$, the allocated fraction of time for power transfer in case of single antenna at any block time is computed as

$$\alpha_i = \frac{P_{\mathcal{R}} d_1^m}{\eta P_S |h_i|^2 + P_{\mathcal{R}} d_1^m}. \tag{9}$$

2.4.2 Dual antennas for energy harvesting

In case of FD communication, the expected relay node is provided with two antennas to receive and transmit signals and such operations are utilized thanks to the collection of RF signal in EH duration. Thus, the received signal at relay node in this stage can be expressed by

$$y_{\mathcal{R},i}^{EH} = \frac{(h_i + k_i)}{\sqrt{d_1^m}} \sqrt{P_S} x_i + n_{\mathcal{R},i}. \tag{10}$$

Similarly, the harvested and transmitted energy regardless of the harvested energy from noise at \mathcal{R} is given by

$$\mathcal{E}_i^{EH} = \eta \alpha_i T \frac{P_S (|h_i|^2 + |k_i|^2)}{d_1^m}. \tag{11}$$

In order to determined EH time, one setting (8) equal to (11), the fraction of time for power transfer in dual

antennas mode for energy harvesting at any block times is determined as

$$\alpha_i = \frac{P_{\mathcal{R}} d_1^m}{\eta P_S (|h_i|^2 + |k_i|^2) + P_{\mathcal{R}} d_1^m}. \tag{12}$$

Remarks 1 In (9) and (12), the duration of time allocated in energy harvesting phase is a function of some variables, including channel gains, optimal power at relay node, the distance between S and \mathcal{R} , i.e. d_1 , energy harvesting coefficient and power transmission at source, i.e. P_S . Specifically, this time fraction is always less than one, i.e., $\alpha_i < 1$, which implies the allocated time which is required for simultaneous wireless information and power transfer.

Remarks 2 Consider energy harvesting time in (9) and (12), to convenience in represent we use two characters α_i^{single} and α_i^{dual} to denote α_i in (9) and (12), respectively. We can observe that, since $|k_i|^2 \geq 0$ and other parameters are invariable then $\alpha_i^{single} \geq \alpha_i^{dual}$. This implies that the time EH with dual antennas is less than that with single antenna. In other words, the amount of WIT time with dual antennas EH case is greater than that with single antenna EH case.

Remarks 3 The proposed modifying TSAC protocol for FD cooperative relaying system is not more require additional time slot since the total frame for communication is as same as [27] (see Remark 1), and the prior installed relay transmit power is a constant value ($P_{\mathcal{R}}$) while the EH time is a function of the random variable WPT channel gain(s) as [31–33].

It is worth noting that the Tables 2 and 3 confirmed that our study aims to find power allocation to obtain optimal performance in energy harvesting networks. Such scheme relies on calculation of CSI feedback signal and so-called offline power allocation due to requiring low complexity in design of real applications.

3 Optimal power allocation for maximized instantaneous throughput

Energy harvesting is an effective method to enhance the performance of the power-constrained relay with available RF signals, in which the transmission power at relay is allocated to maximize the instantaneous throughput. In this paper, the optimal transmitted power in energy harvesting scheme is proposed for FD relay networks.

The instantaneous throughput of FD relay can be expressed by

$$C = (1 - \alpha) \log_2 (1 + \gamma^{e2e}). \tag{13}$$

Table 2 The previous relevant works and their contributions

Reference	EH protocol	Transmission mode	Relay mode	Works area
Nasir et al. [5]	TS, PS	Half duplex	AF	Throughput analysis
Nasir et al. [33]	Continues and discrete TS	Half duplex	AF, DF	Throughput analysis
Chen et al. [17]	Non EH	Full duplex	DF	Optimal power allocation
Zeng and Zhang [28]	TS with energy recycling	Full duplex	AF	Optimizing relay transmission power
Zhong et al. [27]	TS	Full duplex	AF, DF	Optimizing throughput
Ding et al. [32]	Adaptive TS	Half duplex	AF, DF	Optimizing throughput
Ding et al. [15]	PS with storage	Half duplex	DF	Outage performance analysis
Krikidis [16]	PS with storage	Half duplex	DF	Outage performance analysis
Our work	TS aware channel	Full duplex	DF	Optimizing transmit power at relay Throughput analysis.

The optimal transmit power allocated for relay node is formulated as

$$P_{\mathcal{R}}^{opt} = \arg \max_{P_{\mathcal{R}}} \{C(P_{\mathcal{R}})\}, \tag{14}$$

s.t. $0 \leq P_{\mathcal{R}}$.

3.1 Energy harvested by single antenna

Substituting (3), (4), (5), and (9) into (13), the instantaneous throughput is the function of relay transmit power which can be written as follow

$$C(P_{\mathcal{R}}) = \left(1 - \frac{P_{\mathcal{R}}d_1^m}{\eta P_S |h|^2 + P_{\mathcal{R}}d_1^m}\right) \times \log_2 \left(1 + \min \left(\frac{P_S |h|^2}{P_{\mathcal{R}}d_1^m |f|^2 + d_1^m \sigma_{\mathcal{R}}^2}, \frac{P_{\mathcal{R}} |g|^2}{d_2^m \sigma_{\mathcal{D}}^2}\right)\right). \tag{15}$$

Theorem 1 *The optimum transmitted power at the energy-constrained relay for maximizing instantaneous throughput is calculated by*

$$P_{\mathcal{R}}^{opt} = \begin{cases} e^{\frac{\mathcal{W}(\frac{\pi_2 \pi_3 - 1}{e}) + 1}{\pi_2} - 1}, & e^{\mathcal{W}(\frac{\pi_2 \pi_3 - 1}{e}) + 1} < \pi_2 \frac{\sqrt{\Delta} - \pi_0}{2\pi_1} + 1, \\ \frac{\sqrt{\Delta} - \pi_0}{2\pi_1}, & \text{otherwise.} \end{cases} \tag{16}$$

where $\pi_0 = \frac{d_1^m \sigma_{\mathcal{R}}^2}{P_S |h|^2}$, $\pi_1 = \frac{d_1^m |f|^2}{P_S |h|^2}$, $\pi_2 = \frac{|g|^2}{d_2^m \sigma_{\mathcal{D}}^2}$, $\pi_3 = \frac{\eta P_S |h|^2}{d_1^m}$, $\Delta = \pi_0^2 + \frac{4\pi_1}{\pi_2}$, and $\mathcal{W}(x)$ is the Lambert function in [34],

where $\mathcal{W}(x)$ can be found due to the problem solving of $\mathcal{W} \exp(\mathcal{W}) = x$.

Proof Please see in Appendix A. □

3.2 Energy harvested by dual antennas

Similarly, substituting (3), (4), (5), and (12) into (13), the instantaneous throughput can be formulated as below

$$C(P_{\mathcal{R}}) = \left(1 - \frac{P_{\mathcal{R}}d_1^m}{\eta P_S (|h|^2 + |k|^2) + P_{\mathcal{R}}d_1^m}\right) \times \log_2 \left(1 + \min \left(\frac{P_S |h|^2}{P_{\mathcal{R}}d_1^m |f|^2 + d_1^m \sigma_{\mathcal{R}}^2}, \frac{P_{\mathcal{R}} |g|^2}{d_2^m \sigma_{\mathcal{D}}^2}\right)\right). \tag{17}$$

The optimal relay transmission power is derived in the same way as (14).

Theorem 2 *The optimal allocation of transmit power at relay in case of two antennas equipped for EH for maximizing instantaneous mode is given by*

$$P_{\mathcal{R}}^{opt} = \begin{cases} e^{\frac{\mathcal{W}(\frac{\pi_2 \pi_4 - 1}{e}) + 1}{\pi_3} - 1}, & e^{\mathcal{W}(\frac{\pi_2 \pi_4 - 1}{e}) + 1} < \pi_2 \frac{\sqrt{\Delta} - \pi_0}{2\pi_1} + 1, \\ \frac{\sqrt{\Delta} - \pi_0}{2\pi_1}, & \text{otherwise.} \end{cases} \tag{18}$$

where $\pi_4 = \frac{\eta P_S (|h|^2 + |k|^2)}{d_1^m}$ and other related parameters are defined as in Theorem 1.

Table 3 CSI requirement for proposed TSAC protocol schemes

EH type	Transmission mode	CSI requirements	Channel information
Single antennas	Instantaneous	High	$ h_i ^2, g_i ^2, f_i ^2$
Single antennas	Delay-constrained	Medium	$ h_i ^2$, and distributions of $ g_i ^2, f_i ^2$
Dual antennas	Instantaneous	High	$ h_i ^2, k_i ^2, g_i ^2, f_i ^2$
Dual antennas	Delay-constrained	Medium	$ h_i ^2, k_i ^2$, and distributions of $ g_i ^2, f_i ^2$

Proof The Theorem can be explained by using in a similar way to Theorem 1. \square

Remarks 4 *In practical wireless system, only causal channel information and harvested energy are useful in calculation of power allocation. Unfortunately, the offline power allocation policy is not readily applicable in reality. Considering at a given time slot, the CSI in the second hop of the relaying network and the upcoming harvested energy are not known in advance and hence power allocation is evaluated in stochastic circumstance. However, such solution only requires low complexity when comparing online power allocation which is high computational complexity and may not be implementable in practice.*

4 Analysis of outage probability and throughput in delay-constrained transmission mode

In this section, we consider the optimal throughput and outage probability of two-hop relaying networks in FD transmission mode. In this scenario, the system is designed with the fixed transmission rate or the preset SNR threshold γ_0 . In particular, the system suffers from outage when the SNR performance, i.e., γ_i^{e2e} drops below the threshold value. Therefore, the expression of outage probability can be obtained by

$$OP_i = \Pr \{ \gamma_i^{e2e} < \gamma_0 \} = \Pr \{ \min(\gamma_i^{\mathcal{R}}, \gamma_i^{\mathcal{D}}) < \gamma_0 \}, \quad (19)$$

and the expected value of outage probability can be obtained by substituting (3) and (4) into (19).

As aforementioned in protocol description subsection 2.3, since the relay node will harvest a sufficient amount of energy, \mathcal{E}_i , before operating WIT phase, it is noted that the relay be certainly performed because the harvesting energy time is always less than 1, see Remark 1. Therefore, the relay transmit power $P_{\mathcal{R}}$ is a constant value during the transmission duration, see Remark 3. This quantity of power is preset before (such as by technicians). It is worth noting that the $\gamma_i^{\mathcal{R}}, \gamma_i^{\mathcal{D}}$ are independent in term of $P_{\mathcal{R}}$ as in [31–33].

With the fact that such channel is independent to each other, it can be shown that [17, 20]

$$\begin{aligned} E \{ OP_i \} &= 1 - E_{|h_i|^2, |f_i|^2} \left\{ \Pr \left(\gamma_i^{\mathcal{R}} > \gamma_0 \right) \right\} \times E_{|g_i|^2} \left\{ \Pr \left(\gamma_i^{\mathcal{D}} > \gamma_0 \right) \right\} \\ &= 1 - E_{|h_i|^2, |f_i|^2} \left\{ \Pr \left(\frac{P_S |h_i|^2}{P_{\mathcal{R}} d_1^m |f_i|^2 + d_1^m \sigma_{\mathcal{R},i}^2} > \gamma_0 \right) \right\} \\ &\quad \times E_{|g_i|^2} \left\{ \Pr \left(\frac{P_{\mathcal{R}} |g_i|^2}{d_2^m \sigma_{\mathcal{D},i}^2} > \gamma_0 \right) \right\}. \end{aligned} \quad (20)$$

where $E \{ \cdot \}$ is the expectation function.

In the delay-constrained transmission mode, the throughput efficient in the time slot i th, which is the function of outage probability and the EH duration time, can be formulated by

$$\tau_i^{DC} = (1 - OP_i) (1 - \alpha_i). \quad (21)$$

Therefore, the average throughput efficient of system is written by

$$\tau^{DC} = E \{ \tau_i^{DC} \} = E \{ 1 - OP_i \} - E \{ (1 - OP_i) \alpha_i \}. \quad (22)$$

The optimal value of transmit power for throughput optimization can be presented as below

$$\begin{aligned} P_{\mathcal{R}}^{opt} &= \arg \max_{P_{\mathcal{R}}} \{ \tau^{DC} (P_{\mathcal{R}}) \} \\ \text{s.t.} \quad & 0 \leq P_{\mathcal{R}}. \end{aligned} \quad (23)$$

4.1 Energy harvested by single antenna

The system throughput in this case can be determined as (22) and the next theorem is proposed.

Theorem 3 *When the relay uses single antenna to harvest energy, then the average throughput efficient of the system is given by*

$$\begin{aligned} \tau^{DC} &= \exp \left(- \frac{\gamma_0 d_2^m \sigma_{\mathcal{D}}^2}{\lambda_g P_{\mathcal{R}}} \right) \times \left\{ \exp \left(- \frac{\vartheta}{\lambda_h} \right) \left(\frac{\omega \lambda_f}{m_f \lambda_h} + 1 \right)^{-m_f} \right. \\ &\quad - \frac{\chi}{\lambda_h} \exp \left(\frac{\chi}{\lambda_h} \right) \times \left[\exp \left(\frac{m_f (\chi + \vartheta)}{\omega \lambda_f} \right) \right. \\ &\quad \times \text{Ei} \left(- (\chi + \vartheta) \left(\frac{m_f}{\omega \lambda_f} + \frac{1}{\lambda_h} \right) \right) - \text{Ei} \left(- \frac{\chi + \vartheta}{\lambda_h} \right) \left. \right] \\ &\quad \left. - \frac{\chi}{\lambda_h} \exp \left(\frac{m_f \vartheta}{\omega \lambda_f} \right) \sum_{i=1}^{m_f-1} \frac{1}{i!} \left(\frac{m_f}{\omega \lambda_f} \right)^i \times \tau_{31} \right\}, \end{aligned} \quad (24)$$

where $\chi = \frac{P_{\mathcal{R}} d_1^m}{\eta P_S}, \omega = \frac{\gamma_0 P_{\mathcal{R}} d_1^m}{P_S}, \vartheta = \frac{\gamma_0 d_1^m \sigma_{\mathcal{R}}^2}{P_S}, \text{Ei}$ is the exponential integral function as (Eq. 8.211) in [35], and

$$\begin{aligned} \tau_{31} &\triangleq (-1)^{i+1} \vartheta^i \exp \left(\frac{\chi}{\lambda_h} \right) \text{Ei} \left(- (\chi + \vartheta) \left(\frac{1}{\lambda_h} + \frac{m_f}{\omega \lambda_f} \right) \right) \\ &\quad + \sum_{k=1}^i \binom{i}{k} (-1)^i \vartheta^{i-k} \int_{\vartheta}^{\infty} \exp \left(-x \left(\frac{1}{\lambda_h} + \frac{m_f}{\omega \lambda_f} \right) \right) \frac{x^k}{x + \chi} dx. \end{aligned}$$

Proof The detailed explanation of the Theorem 3 is provided in Appendix B. \square

Alternatively, we can use the following closed-form when the SI channel modeled by Rayleigh fading as following corollary.

Corollary 1 *When $m_f = 1$ (or the SI link at relay experience Rayleigh fading model) the throughput performance in case of single antenna for EH at relay node is given as*

$$\begin{aligned} \tau^{DC} = & \exp\left(-\frac{\gamma_0 d_2^m \sigma_D^2}{\lambda_g P_{\mathcal{R}}}\right) \times \left\{ \exp\left(-\frac{\vartheta}{\lambda_h}\right) \frac{\lambda_h}{\lambda_h + \omega \lambda_f} \right. \\ & + \frac{\chi}{\lambda_h} \exp\left(\frac{\chi}{\lambda_h}\right) \text{Ei}\left(-\frac{\chi + \vartheta}{\lambda_h}\right) \\ & \left. - \frac{\chi}{\lambda_h} \exp\left(\frac{\chi + \vartheta}{\omega \lambda_f} + \frac{\chi}{\lambda_h}\right) \text{Ei}\left(-\frac{\chi + \vartheta}{\omega \lambda_f} - \frac{\chi + \vartheta}{\lambda_h}\right) \right\}. \end{aligned} \quad (25)$$

Proof The Corollary 1 can be obtained easily by substituting $m_f = 1$ into the expression in Theorem 3. \square

Extracting (23) by using (24), the optimal transfer power at relay with the aim of optimizing the system throughput can be obtained. Since $\tau_{DC}(P_{\mathcal{R}})$ is a concave function of $P_{\mathcal{R}}$, the optimal value $P_{\mathcal{R}}^{opt}$ can be obtained by solving the equation $\partial \tau_{DC}(P_{\mathcal{R}})/\partial P_{\mathcal{R}} = 0$. Although the derivation of closed-form optimal expressions is challenging, the optimal value can be obtained by using numerical simulations which are presented in the next section.

4.2 Energy harvested by dual antennas

In this case, we also study the throughput in the delay-constrained mode with the following theorem.

Theorem 4 *We consider a cooperative scenario with two-hop source-relay-destination pair and two antennas provided at energy harvesting relays, the throughput can be determined as*

$$\begin{aligned} \tau^{DC} = & \exp\left(-\frac{\gamma_0 d_2^m \sigma_D^2}{\lambda_g P_{\mathcal{R}}}\right) \times \left\{ \exp\left(-\frac{\vartheta}{\lambda_h}\right) \left(\frac{\omega \lambda_f}{m_f \lambda_h} + 1\right)^{-m_f} \right. \\ & - \frac{\chi}{\lambda_h} \exp\left(\frac{\chi}{\lambda_k}\right) \times \left\{ \lambda_k \exp\left(-\frac{\vartheta + \chi}{\lambda_k}\right) + (\vartheta + \chi) \text{Ei}\left(-\frac{\vartheta + \chi}{\lambda_k}\right) \right. \\ & \times \frac{\omega \lambda_f}{m_f} \text{Ei}\left(-\frac{\vartheta + \chi}{\lambda_k}\right) - \frac{\omega \lambda_f}{m_f} \exp\left(\frac{m_f(\vartheta + \chi)}{\omega \lambda_f}\right) \\ & \left. \left. \times \text{Ei}\left(-(\vartheta + \chi)\left(\frac{1}{\lambda_k} + \frac{m_f}{\omega \lambda_f}\right)\right) \right\} + \exp\left(\frac{m_f(\vartheta + \chi)}{\omega \lambda_f}\right) \times \tau_{43} \right\}, \end{aligned} \quad (26)$$

where χ , ω , ϑ , Ei is defined below Theorem 3, and

$$\begin{aligned} \tau_{43} \triangleq & \sum_{i=1}^{m_f-1} \frac{1}{i!} \left(\frac{m_f}{\omega \lambda_f}\right)^i \left\{ (-1)^i (\vartheta + \chi)^i \frac{\omega \lambda_f \lambda_h}{\omega \lambda_f + m_f \lambda_h} \right. \\ & \times \left[\exp\left(-\left(\frac{1}{\lambda_h} + \frac{m_f}{\omega \lambda_f}\right)(\vartheta + \chi)\right) \text{E}_1\left(\frac{\vartheta + \chi}{\lambda_k}\right) \right. \\ & \left. - \text{E}_1\left((\vartheta + \chi)\left(\frac{1}{\lambda_k} + \frac{1}{\lambda_h} + \frac{m_f}{\omega \lambda_f}\right)\right) \right] \\ & + \sum_{k=1}^i \binom{i}{k} (-\vartheta + \chi)^{i-k} \int_{\vartheta + \chi}^{\infty} t^k \exp\left(-x\left(\frac{1}{\lambda_h} + \frac{m_f}{\omega \lambda_f}\right)\right) \\ & \left. \times \text{E}_1\left(\frac{t}{\lambda_k}\right) dx \right\}. \end{aligned}$$

Proof Please see in Appendix C. \square

When the SI channel is modeled by Rayleigh fading connection, the throughput performance of system is given as corollary below.

Corollary 2 *When $m_f = 1$ (or the SI link at relay experience Rayleigh fading model) the throughput performance in case of dual antenna for EH at relay node is given as*

$$\begin{aligned} \tau^{DC} = & \exp\left(-\frac{\gamma_0 d_2^m \sigma_D^2}{\lambda_g P_{\mathcal{R}}}\right) \times \left\{ \exp\left(-\frac{\vartheta}{\lambda_h}\right) \frac{\lambda_h}{\lambda_h + \omega \lambda_f} \right. \\ & - \frac{\chi}{\lambda_h} \exp\left(\frac{\chi}{\lambda_k}\right) \times \left[\lambda_k \exp\left(-\frac{\vartheta + \chi}{\lambda_k}\right) \right. \\ & + (\vartheta + \chi) \text{Ei}\left(-\frac{\vartheta + \chi}{\lambda_k}\right) \\ & - \omega \lambda_f \left(\exp\left(\frac{\vartheta + \chi}{\omega \lambda_f}\right) \text{Ei}\left(-\frac{\vartheta + \chi}{\lambda_k} - \frac{\vartheta + \chi}{\omega \lambda_f}\right) \right. \\ & \left. \left. - \text{Ei}\left(-\frac{\vartheta + \chi}{\lambda_k}\right) \right) \right] \right\}. \end{aligned} \quad (27)$$

Proof It is easy to obtain the Corollary 2 by substituting $m_f = 1$ into the expression in Theorem 4. \square

Remarks 5 *Regarding impact of self-interference (SI) cancellation, the active SI suppression methods were shown experimentally to be capable of facilitating FD at short range communication. To apply energy harvesting in a real FD system, it is critical to accurately measure and suppress the SI in such FD networks. In this paper, we investigate SI in system performance through numerical simulation results.*

5 Half-duplex relaying networks

In HD transmission mode, the relay node uses single antenna for energy harvesting and information processing. In order to compare with the FD relaying systems, we consider different transmission modes. Some of the results have been derived in [31–33]; however, we present here to make our work self-contained.

In this scenario, the received signal at relay in HD mode is presented as

$$y_{\mathcal{R},i} = \frac{h_i}{\sqrt{d_1^m}} \sqrt{P_S} x_i + n_{\mathcal{R},i}, \quad (28)$$

And the SNR at relay node given by

$$\gamma_i^{\mathcal{R}} = \frac{P_S |h_i|^2}{d_1^m \sigma_{\mathcal{R},i}^2}. \quad (29)$$

5.1 Instantaneous transmission mode

In this scenario, the instantaneous throughput can be illustrated as

$$C_{HD} = \frac{1}{2} (1 - \alpha) \log_2 (1 + \gamma^{e2e}). \quad (30)$$

The optimal allocation for power transmission at relay is similar to (14)

Theorem 5 *The optimal power allocation in HD relaying networks for instantaneous transmission mode can be calculated as*

$$P_{\mathcal{R}}^{opt} = \begin{cases} e^{\frac{\mathcal{W}\left(\frac{2\pi_2\theta-1}{e}\right)+1}{\pi_2}} - 1, & e^{\mathcal{W}\left(\frac{2\pi_2\theta-1}{e}\right)+1} < \frac{1}{\pi_0} + 1, \\ \frac{1}{\pi_0\pi_2}, & \text{otherwise.} \end{cases} \quad (31)$$

where $\theta = \pi_3$ in case of single antenna, $\theta = \pi_4$ in case of dual antennas. And $\pi_0, \pi_2, \pi_3, \pi_4$ are defined as below Theorem 1.

Proof The proof is similar to that of Theorem 1. \square

5.2 Delay-constrained transmission mode

The throughput of HD relaying can be obtained as

$$\tau_i^{DC} = \frac{1}{2} (1 - OP_i) (1 - \alpha_i). \quad (32)$$

In comparison with the calculation of throughput in FD mode, in (21), the factor 2 can be seen by the denominator denoting as transmission efficiency. In following calculation, we can obtain two theorem which are solved similarly as that in Theorem 4.

Theorem 6 *In the HD mode relaying, the throughput in case of single antenna given by*

$$\tau^{HD} = \frac{1}{2} \exp\left(-\frac{\gamma_0^{HD} d_2^m \sigma_D^2}{\lambda_g P_{\mathcal{R}}}\right) \times \left\{ \exp\left(-\frac{\gamma_0^{HD} d_1^m \sigma_{\mathcal{R}}^2}{\lambda_h P_S}\right) + \frac{\chi_1}{\lambda_h} \exp\left(\frac{\chi_1}{\lambda_h}\right) \text{Ei}\left(-\frac{(\chi_1 + \vartheta_1)}{\lambda_h}\right) \right\}. \quad (33)$$

Theorem 7 *In case that the energy is harvested by dual antennas, the throughput of HD relaying networks can be determined as*

$$\tau^{HD} = \frac{1}{2} \exp\left(-\frac{\gamma_0^{HD} d_2^m \sigma_D^2}{\lambda_g P_{\mathcal{R}}}\right) \left\{ \exp\left(-\frac{\gamma_0^{HD} d_1^m \sigma_{\mathcal{R}}^2}{\lambda_h P_S}\right) - \frac{\chi_1}{\lambda_h \lambda_k} \exp\left(\frac{\chi_1}{\lambda_k}\right) \times \left[\lambda_k \exp\left(-\frac{\vartheta_1 + \chi_1}{\lambda_k}\right) + (\vartheta_1 + \chi_1) \text{Ei}\left(-\frac{\vartheta_1 + \chi_1}{\lambda_k}\right) \right] \right\}, \quad (34)$$

where $\chi_1 = \frac{P_{\mathcal{R}} d_1^m}{2\eta P_S}, \vartheta_1 = \frac{\gamma_0^{HD} d_1^m \sigma_{\mathcal{R}}^2}{P_S}$.

6 Numerical results

In this section, numerical simulation results are demonstrated to validate analytical expressions as concerns in the previous section, and the impact of key system parameters is investigated in detail in terms of system throughput. The energy harvesting efficiency is set $\eta = 0.8$, while the path loss exponent is set $m = 3$. The distances, d_1 and d_2 are normalized values which are set $d_1 = 3$ and $d_2 = 1$, respectively. The simulation environments are associated with the detailed parameters as $\gamma_0 = 10$ dB, $\lambda_f = 0.01, \lambda_h = 1, \lambda_k = 1, \lambda_g = 1, P_S = 26$ dB and noise terms as $\sigma_D^2 = -5$ dB, $\sigma_{\mathcal{R}}^2 = -10$ dB. In this subsection, we present simulation results to verify the analytical results. The throughput performance is calculated by averaging the throughput values over a 100,000 blocks, while fading channels for each block is perfectly independent.

Figure 3 illustrates the impact of received power at relay node on the instantaneous throughput. To compare the performance of FD and HD relay, we set $|f|^2 = 0.05, |h|^2 = 1.2, |g|^2 = 1.4, |k|^2 = 1$. The figure proves that the analytical results based on curves match well with the simulation results. It is noted that the optimal received power at relay for single antenna in HD case and FD case is smaller than those schemes with dual antennas, and the highest instantaneous throughput of FD case outperforms the HD case. When the received power is small, more energy can be collected to facilitate the information transmission while more received power or strong loop-back interference is produced such as the excessive amount of harvested energy, which is the primary cause of worse system performance.

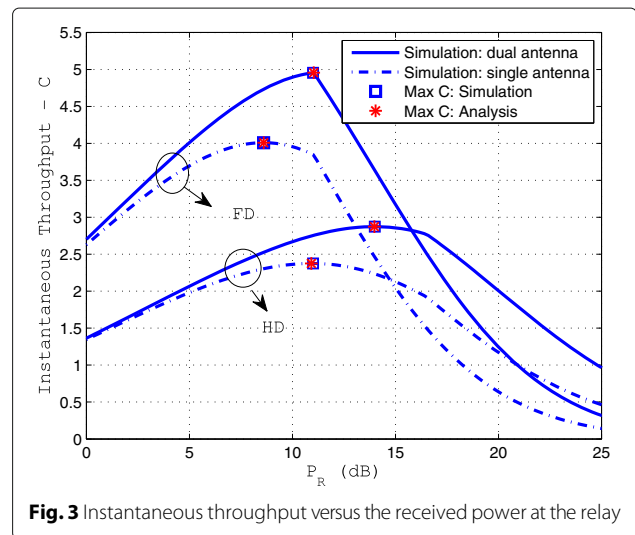


Fig. 3 Instantaneous throughput versus the received power at the relay

The average throughput in delay constraint mode is presented in Fig. 4. It can be observed that the dual antenna case outperforms the single antenna case in terms of the received power at relay. In fact, the dual antennas case can harvest more energy with less transmit power. However, when the transmit power is larger than the optimal harvested power, it results in lower average throughput caused by loop-back interference. On the other hand, the gap between throughput of single antenna and dual antennas is still trivial due to short time for energy harvesting. In general, there should be a balance between energy harvesting capability and noise processing. One can increase P_R to the optimal value, at approximately 10 dB to achieve optimal throughput. As the previous illustration, it is confirmed that FD relay is better than HD relay when the received power at relay is small.

Next, it can be observed that throughput performance improves as increasing transmit power of the source node as in Fig. 5. To evaluate the impacts of the factor m_f in Nakagami channel of SI on system performance, in this experience we set $\lambda_f = 0.1$ and $P_R = P_S - 10$ (dB). The smallest of m_f brings the highest throughput performance. A general observation is that the dual antenna model significantly outperforms the single antenna counterpart at any values of transmit power of the source. Interestingly, when the transmit power overcome about 40 dB, the throughput still remain the peak value in stable floor.

To illustrate the impact of noise variance at relay and destination node in case of optimal throughput, Figs. 6 and 7 also show that dual antennas in FD mode outperform FD single antenna. This can be explained as follows: A lower noise variance decreases the outage probability and hence we obtain more throughput. Conversely, as for higher noise variance, the outage probability increases while the throughput falls dramatically. Thus, the system

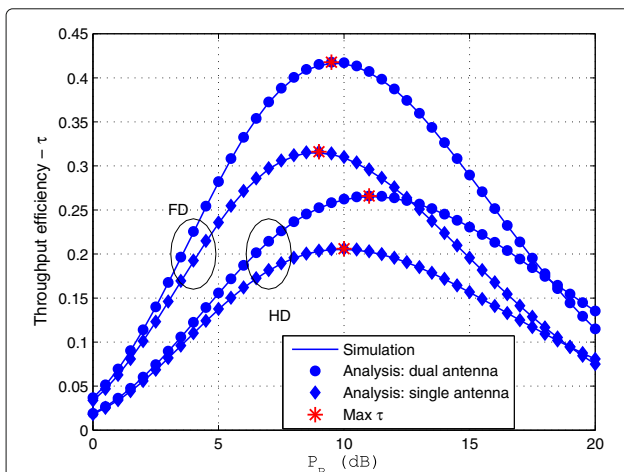


Fig. 4 Throughput efficiency versus P_R in FD relay with $m_f = 1$

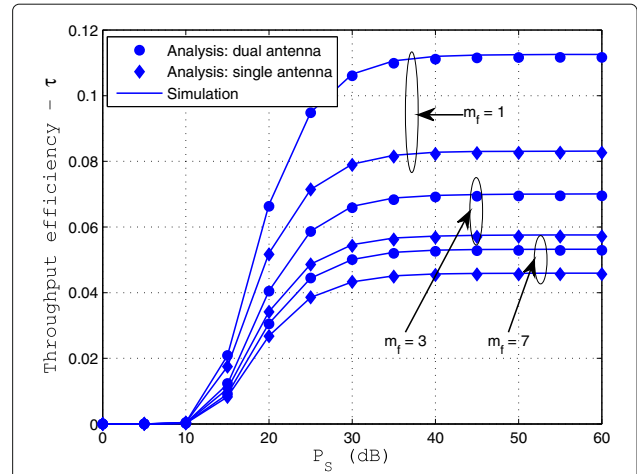


Fig. 5 Throughput efficiency versus P_S with difference case of m_f , $\lambda_f = 0.1$ and $P_R = P_S - 10$ (dB)

performance is affected more by erroneous information processing, leading to a waste of resources during the whole block time. In addition, it can be seen that the impact of noise term at relay affects the noise term at destination more. As a result, throughput performance in Fig. 7 declines sharply when noise varies from -5 to 5 dB.

In Fig. 8, the simulation results present the throughput efficiency versus γ_0 and compare with existing protocols in [27] and [28]. The main observation is the effect of threshold SNR on throughput in delay constraint mode using TSAC, which is investigated with different quantities of antennas, especially in comparison with traditional energy harvesting protocols. The simulation parameters are installed as $\alpha = 0.2$, $P_R = 10$ dB. The throughput in case of TSAC is better than the traditional case due to optimal time for energy harvesting which is solved in

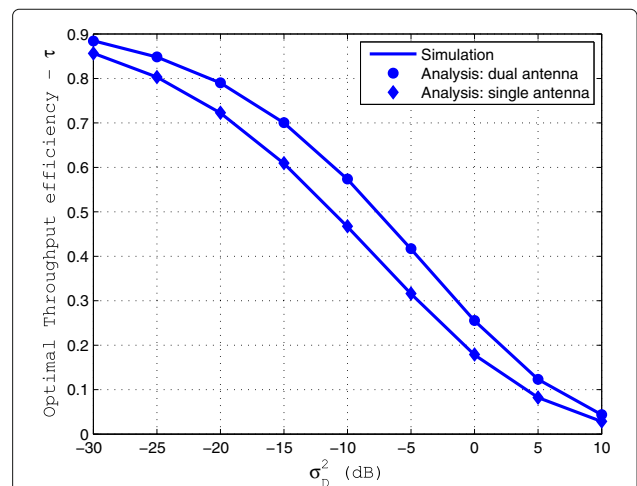
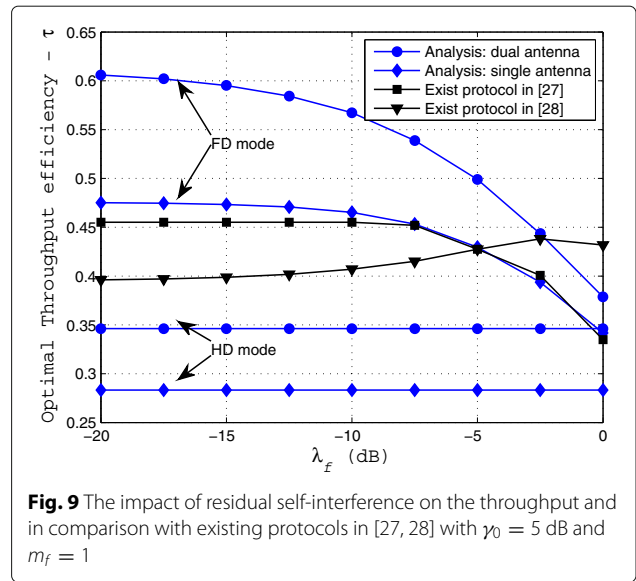
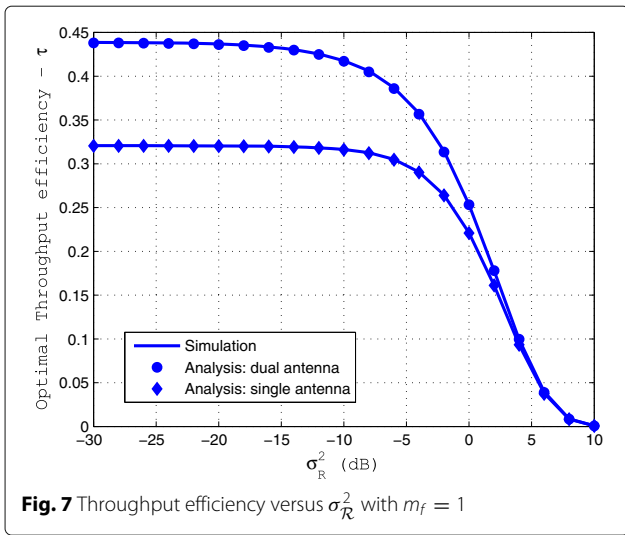


Fig. 6 Throughput efficiency versus σ_D^2 with $m_f = 1$

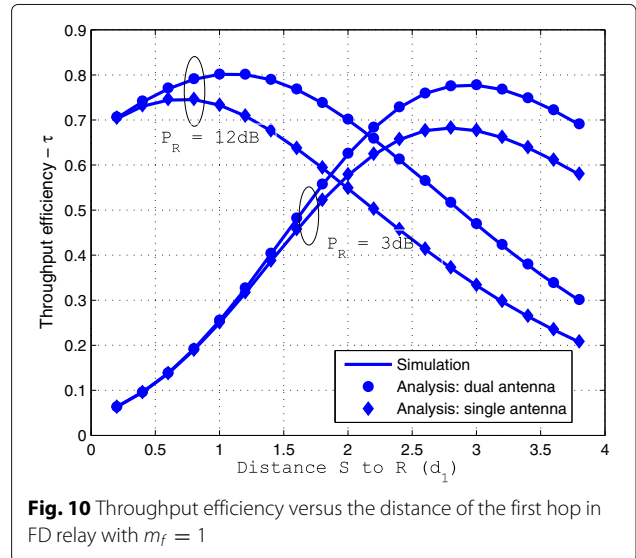
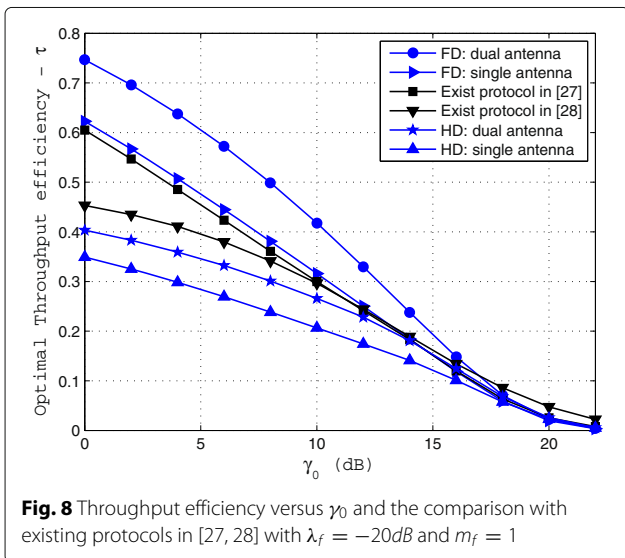


the proposed TSAC. In case of γ_0 described below 14 dB, the proposed protocol related to the optimal throughput efficiency outperforms the existing protocols. However, in high threshold regime, the self-energy recycling protocol proposed in [28] is slightly better than those schemes. In general, this figure reveals that the FD relay has worse performance at higher threshold SNR, which means the system may require higher bit per channel.

As depicted in Fig. 9, the dual antenna FD relay based on TSAC outperforms the single antenna in terms of residual self-interference. When the residual self-interference is greater than -5 dB, throughput decreases significantly, since this loop-back noise impairs the overall performance. Therefore, the self-interference should be remained lower than acceptable value to satisfy system performance and the FD transmission is only beneficial, if

the loop-back noise is eliminated. When SI factor ranges from -20 to -5 dB, the performance of TSAC scheme is superior to the existing protocols, but when SI parameters are greater than -5 dB, the optimal throughput of the proposed protocol in [28] is a prime candidate. Thanks to the EH protocol proposed in [28], the loop interference at relay is reused for self-energy recycling. As a result, part of the energy (loop energy) is used for information transmission by the relay and it improves the scheme's performance.

According to Fig. 10, the throughput changes dramatically when we move the relay node in several positions between the source and destination node. The results are then obtained by setting $d_1 = 0.2 \rightarrow 3.8$, $d_2 = 4 - d_1$.



The distance between relay and source has a capability of energy harvesting which can illustrate how much energy can be obtained via wireless channel. It can be seen clearly that opposite trends for optimal throughput with the received power at relay, $P_{\mathcal{R}} = 3$ dB and $P_{\mathcal{R}} = 12$ dB.

7 Conclusion

In this paper, the throughput of FD and HD relaying in RF energy harvesting systems is investigated. Interestingly, the number of antennas equipped at each relay has significant influence to throughput performance due to the harvested energy at the relay node. Regarding optimal throughput, analytical expressions for the outage probability and throughput capacity of the system were derived. Therefore, the optimal time switching of energy harvesting was comprehensively evaluated. It is confirmed that by employing dual antennas at relay for energy harvesting is beneficial, and the throughput gain is significant when transmit power at source and the received power at relay are carefully calculated. In addition, in comparison with HD relaying networks, our results indicate that FD relaying can substantially boost the system throughput with optimal power allocation policy at energy harvesting-enabled relay. Via mathematical and numerical analysis, the optimal throughput in both instantaneous transmission mode and delay constraint transmission mode can be obtained. More importantly, in order to compute optimal time switching fractions in energy harvesting protocol so-called TSAC, it solely relies on the channel statistics without the need of instantaneous CSI, and it has become an attractive solution to implement in future RF energy harvesting cooperative systems. Finally, for enhancing energy harvesting efficiency, future works should take into account the extra energy with multiple antenna system model (MIMO) to transmit wireless power.

Appendix

A Proof of Theorem 1

Setting $\pi_0 = \frac{d_1^m \sigma_{\mathcal{R}}^2}{P_S |h|^2}$ and $\pi_1 = \frac{d_1^m |f|^2}{P_S |h|^2}$, $\pi_2 = \frac{|g|^2}{d_2^m \sigma_{\mathcal{D}}^2}$, $\pi_3 = \frac{\eta P_S |h|^2}{d_1^m}$, the formula (15) can be re-expressed as

$$C(P_{\mathcal{R}}) = \left(1 - \frac{P_{\mathcal{R}}}{\pi_3 + P_{\mathcal{R}}}\right) \times \log_2 \left(1 + \min \left(\frac{1}{\pi_0 + \pi_1 P_{\mathcal{R}}}, \pi_2 P_{\mathcal{R}}\right)\right). \tag{35}$$

In (35), two cases can be calculated as below

$$C(P_{\mathcal{R}}) = \begin{cases} \frac{\pi_3}{\pi_3 + P_{\mathcal{R}}} \log_2 (1 + \pi_2 P_{\mathcal{R}}), & \text{if } \pi_2 P_{\mathcal{R}} < \frac{1}{\pi_0 + \pi_1 P_{\mathcal{R}}}, \\ \frac{\pi_3}{\pi_3 + P_{\mathcal{R}}} \log_2 \left(1 + \frac{1}{\pi_0 + \pi_1 P_{\mathcal{R}}}\right), & \text{otherwise.} \end{cases} \tag{36}$$

In case $\pi_2 P_{\mathcal{R}} < \frac{1}{\pi_0 + \pi_1 P_{\mathcal{R}}}$ and combine the power at relay, e.g $P_{\mathcal{R}}$, is the non-negative number, we achieve $0 \leq P_{\mathcal{R}} < \frac{\sqrt{\Delta} - \pi_0}{2\pi_1}$.

Taking the derivative of $C(P_{\mathcal{R}})$ with respect to $P_{\mathcal{R}}$ and setting equal zero, we have

$$\frac{\pi_2}{1 + \pi_2 P_{\mathcal{R}}} = \frac{\ln(1 + \pi_2 P_{\mathcal{R}})}{\pi_3 + P_{\mathcal{R}}}. \tag{37}$$

After some algebraic manipulations, we have

$$\frac{\pi_2 \pi_3 - 1}{e} = \exp \left\{ \ln \left(\frac{1 + \pi_2 P_{\mathcal{R}}}{e} \right) \right\} \ln \left(\frac{1 + \pi_2 P_{\mathcal{R}}}{e} \right). \tag{38}$$

Using the form of Lambert function, (38) can be written as

$$\ln \left(\frac{1 + \pi_2 P_{\mathcal{R}}}{e} \right) = \mathcal{W} \left(\frac{\pi_2 \pi_3 - 1}{e} \right). \tag{39}$$

With (39), after some algebraic manipulations, we get

$$P_{\mathcal{R}}^{opt} = \frac{e^{\mathcal{W} \left(\frac{\pi_2 \pi_3 - 1}{e} \right) + 1} - 1}{\pi_2}. \tag{40}$$

In case 2, where $\frac{1}{\pi_0 + \pi_1 P_{\mathcal{R}}} \leq \pi_2 P_{\mathcal{R}}$ or $P_{\mathcal{R}} \geq \frac{\sqrt{\Delta} - \pi_0}{2\pi_1}$ the instantaneous throughput is $C(P_{\mathcal{R}}) = \log_2 \left(1 + \frac{1}{\pi_0 + \pi_1 P_{\mathcal{R}}}\right) \frac{\pi_3}{\pi_3 + P_{\mathcal{R}}}$. Getting the first coefficient of throughput, $C(P_{\mathcal{R}})$ with respect of $P_{\mathcal{R}}$ variable, we have

$$\frac{\partial \{C(P_{\mathcal{R}})\}}{\partial P_{\mathcal{R}}} = -\frac{\pi_0}{(\pi_3 + P_{\mathcal{R}})^2} \log_2 \left(1 + \frac{1}{\pi_0 + \pi_1 P_{\mathcal{R}}}\right) - \frac{1}{\ln(2)} \frac{\pi_1}{(\pi_0 + \pi_1 P_{\mathcal{R}})(\pi_0 + \pi_1 P_{\mathcal{R}} + 1)} \frac{\pi_3}{\pi_3 + P_{\mathcal{R}}}. \tag{41}$$

In (41), the derivative expression involves a negative value. Hence, $C(P_{\mathcal{R}})$ is the restrictive function with the increase in variable, $P_{\mathcal{R}}$. Therefore, the optimal power can be obtained as

$$P_{\mathcal{R}}^{opt} = \frac{\sqrt{\Delta} - \pi_0}{2\pi_1}. \tag{42}$$

This is end of proof.

B Proof of Theorem 3

Substituting (9), (20) into (22), then putting $\chi = \frac{P_{\mathcal{R}} d_1^m}{\eta P_S}$, $\omega = \frac{\gamma_0 P_{\mathcal{R}} d_1^m}{P_S}$ and $\vartheta = \frac{\gamma_0 d_1^m \sigma_{\mathcal{R}}^2}{P_S}$, as thus the average throughput of system can be expressed

$$\tau^{DC} = E_{|g_i|^2} \left\{ \underbrace{\Pr \left(\frac{P_{\mathcal{R}} |g_i|^2}{d_2^m \sigma_{\mathcal{D},i}^2} > \gamma_0 \right)}_{\tau_1^{DC}} \times \left\{ \underbrace{E_{|h_i|^2, |f_i|^2} \left\{ \Pr \left(|h_i|^2 > \omega |f_i|^2 + \vartheta \right) \right\}}_{\tau_2^{DC}} - \underbrace{E_{|h_i|^2, |f_i|^2} \left\{ \Pr \left(|h_i|^2 > \omega |f_i|^2 + \vartheta \right) \frac{\chi}{|h_i|^2 + \chi} \right\}}_{\tau_3^{DC}} \right\} \right\}. \tag{43}$$

The first item could be evaluated with the fact that the $|g_i|^2$ channel experience exponential distribution, yields

$$\begin{aligned} \tau_1^{DC} &= E_{|g_i|^2} \left\{ \Pr \left(P_{\mathcal{R}} |g_i|^2 > \gamma_0 d_2^m \sigma_{\mathcal{D}}^2 \right) \right\} \\ &= F_{|g_i|^2} \left(\frac{\gamma_0 d_2^m \sigma_{\mathcal{D}}^2}{\lambda_g P_{\mathcal{R}}} \right) = \exp \left(- \frac{\gamma_0 d_2^m \sigma_{\mathcal{D}}^2}{\lambda_g P_{\mathcal{R}}} \right), \end{aligned} \tag{44}$$

where $F_X(x)$ is the cumulative distribution function (cdf) function of random variable X .

And the second item can be obtained as

$$\begin{aligned} \tau_2^{DC} &\triangleq E_{|h_i|^2, |f_i|^2} \left\{ \Pr \left(|h_i|^2 > \omega |f_i|^2 + \vartheta \right) \right\} \\ &= \int_0^\infty F_{|h_i|^2}(\omega x + \vartheta) f_{|f_i|^2}(x) dx \\ &\stackrel{(a)}{=} \exp \left(- \frac{\vartheta}{\lambda_h} \right) \frac{m_f}{\Gamma(m_f) \lambda_f^{m_f}} \int_0^\infty x^{m_f-1} \exp \left(-x \left(\frac{\omega}{\lambda_h} + \frac{m_f}{\lambda_f} \right) \right) dx \\ &\stackrel{(b)}{=} \exp \left(- \frac{\vartheta}{\lambda_h} \right) \left(\frac{\omega \lambda_f}{m_f \lambda_h} + 1 \right)^{-m_f}, \end{aligned} \tag{45}$$

where $f_X(x)$ is the pdf of random variable X , step (a) is done by $|f_i|^2$ following the gamma distribution and $|h_i|^2$ experience exponential distribution, stage (b) is revealed by using (eq. 3.381.4) in [35].

Finally, the third element is determined as

$$\begin{aligned} \tau_3 &\triangleq E_{|h_i|^2, |f_i|^2} \left\{ \Pr \left(\omega |f_i|^2 < |h_i|^2 - \vartheta \right) \frac{\chi}{|h_i|^2 + \chi} \right\} \\ &= \int_{\vartheta}^\infty \frac{\chi}{x + \chi} F_{|f_i|^2} \left(\frac{x - \vartheta}{\omega} \right) f_{|h_i|^2}(x) dx \\ &= \frac{\chi}{\lambda_h} \int_{\vartheta}^\infty \exp \left(- \frac{x}{\lambda_h} \right) \left(1 - \exp \left(- \frac{m_f (x - \vartheta)}{\omega \lambda_f} \right) \right) \\ &\quad \times \sum_{i=0}^{m_f-1} \frac{1}{i!} \left(\frac{m_f}{\omega \lambda_f} \right)^i (x - \vartheta)^i \frac{1}{x + \chi} dx \\ &\stackrel{(a)}{=} \frac{\chi}{\lambda_h} \left\{ - \exp \left(\frac{\chi}{\lambda_h} \right) \text{Ei} \left(- \frac{\chi + \vartheta}{\lambda_h} \right) + \exp \left(\frac{\chi}{\lambda_h} \right) \exp \left(\frac{m_f (\chi + \vartheta)}{\omega \lambda_f} \right) \right. \\ &\quad \times \text{Ei} \left(- (\chi + \vartheta) \left(\frac{m_f}{\omega \lambda_f} + \frac{1}{\lambda_h} \right) \right) - \exp \left(\frac{m_f \vartheta}{\omega \lambda_f} \right) \sum_{i=1}^{m_f-1} \frac{1}{i!} \left(\frac{m_f}{\omega \lambda_f} \right)^i \\ &\quad \left. \times \int_{\vartheta}^\infty \exp \left(-x \left(\frac{1}{\lambda_h} + \frac{m_f}{\omega \lambda_f} \right) \right) \frac{(x - \vartheta)^i}{x + \chi} dx \right\}, \end{aligned} \tag{46}$$

where the step (a) can be derived by applying given in ([35], Eq. 3.352.2). The last item in (46) can be reduced as

$$\begin{aligned} \tau_{31} &\triangleq (-1)^i \vartheta^i \int_{\vartheta}^\infty \exp \left(-x \left(\frac{1}{\lambda_h} + \frac{m_f}{\omega \lambda_f} \right) \right) \frac{1}{x + \chi} dx \\ &\quad + \sum_{k=1}^i \binom{i}{k} (-1)^i \vartheta^{i-k} \int_{\vartheta}^\infty \exp \left(-x \left(\frac{1}{\lambda_h} + \frac{m_f}{\omega \lambda_f} \right) \right) \frac{x^k}{x + \chi} dx \\ &= (-1)^{i+1} \vartheta^i \exp \left(\frac{\chi}{\lambda_h} \right) \text{Ei} \left(- (\chi + \vartheta) \left(\frac{1}{\lambda_h} + \frac{m_f}{\omega \lambda_f} \right) \right) \\ &\quad + \sum_{k=1}^i \binom{i}{k} (-1)^i \vartheta^{i-k} \int_{\vartheta}^\infty \exp \left(-x \left(\frac{1}{\lambda_h} + \frac{m_f}{\omega \lambda_f} \right) \right) \frac{x^k}{x + \chi} dx. \end{aligned} \tag{47}$$

Substituting (44), (45), (46), and (47) into (43), Theorem 3 is simply derived. This ends the proof.

C Proof of Theorem 4

Substituting (12), (20), into (22) the average throughput of system can be expressed

$$\tau^{DC} = E_{|g_i|^2} \left\{ \underbrace{\Pr \left(\frac{P_{\mathcal{R}} |g_i|^2}{d_2^m \sigma_{D,i}^2} > \gamma_0 \right)}_{\tau_1^{DC}} \right. \\ \times \left. \left\{ \underbrace{E_{|h_i|^2, |f_i|^2} \left\{ \Pr \left(|h_i|^2 > \omega |f_i|^2 + \vartheta \right) \right\}}_{\tau_2^{DC}} \right. \right. \\ \left. \left. - \underbrace{E_{|h_i|^2, |f_i|^2, |k_i|^2} \left\{ \Pr \left(|h_i|^2 > \omega |f_i|^2 + \vartheta \right) \frac{\chi}{|h_i|^2 + |k_i|^2 + \chi} \right\}}_{\tau_4^{DC}} \right\} \right\}. \tag{48}$$

The first and second elements (i.e. τ_1^{DC} , τ_2^{DC}) can be obtained as (44), (45) in Appendix 7, respectively. And the third item can be expressed as

$$\tau_4^{DC} \triangleq \int_{|h_i|^2, |f_i|^2, |k_i|^2} \left\{ \Pr \left(\omega |f_i|^2 < |h_i|^2 - \vartheta \right) \frac{\chi}{|k_i|^2 + |h_i|^2 + \chi} \right\} \\ = \int_{\vartheta}^{\infty} F_{|f_i|^2} \left(\frac{x - \vartheta}{\omega} \right) f_{|h_i|^2}(x) \int_0^{\infty} \frac{\chi}{t + x + \chi} f_{|k_i|^2}(t) dt dx \\ = \frac{\chi}{\lambda_h} \int_{\vartheta}^{\infty} F_{|f_i|^2} \left(\frac{x - \vartheta}{\omega} \right) \exp \left(-\frac{x}{\lambda_h} \right) \exp \left(\frac{x + \chi}{\lambda_k} \right) E_1 \left(\frac{x + \chi}{\lambda_k} \right) dx \\ = \frac{\chi}{\lambda_h} \exp \left(\frac{\chi}{\lambda_k} \right) \times \left\{ \tau_{41} - \exp \left(\frac{m_f (\vartheta + \chi)}{\omega \lambda_f} \right) \times (\tau_{42} + \tau_{43}) \right\}, \tag{49}$$

in which the terms τ_{41} and τ_{42} can be derived as

$$\tau_{41} \triangleq \int_{\vartheta + \chi}^{\infty} E_1 \left(\frac{t}{\lambda_k} \right) dt = \int_0^{\infty} E_1 \left(\frac{t}{\lambda_k} \right) dt - \int_0^{\vartheta + \chi} E_1 \left(\frac{t}{\lambda_k} \right) dt \\ = \lambda_k \exp \left(-\frac{\vartheta + \chi}{\lambda_k} \right) + (\vartheta + \chi) E_1 \left(\frac{\vartheta + \chi}{\lambda_k} \right). \tag{50}$$

The integral can be derived with help of (Eq. 5.221.8) and (Eq. 6.224.1) given in [35] and

$$\tau_{42} \triangleq \int_{\vartheta + \chi}^{\infty} \exp \left(-\frac{m_f t}{\omega \lambda_f} \right) E_1 \left(\frac{t}{\lambda_k} \right) dt \\ = \int_0^{\infty} \exp \left(-\frac{m_f t}{\omega \lambda_f} \right) E_1 \left(\frac{t}{\lambda_k} \right) dt - \int_0^{\vartheta + \chi} \exp \left(-\frac{m_f t}{\omega \lambda_f} \right) E_1 \left(\frac{t}{\lambda_k} \right) dt \\ = \frac{\omega \lambda_f}{m_f} \left\{ \exp \left(-\frac{m_f (\vartheta + \chi)}{\omega \lambda_f} \right) E_1 \left(\frac{\vartheta + \chi}{\lambda_k} \right) \right. \\ \left. - E_1 \left((\vartheta + \chi) \left(\frac{1}{\lambda_k} + \frac{m_f}{\omega \lambda_f} \right) \right) \right\}, \tag{51}$$

and

$$\tau_{43} \triangleq \int_{\vartheta + \chi}^{\infty} \exp \left(-\frac{m_f t}{\omega \lambda_f} \right) \sum_{i=1}^{m_f-1} \frac{1}{i!} \left(\frac{m_f}{\omega \lambda_f} \right)^i (t - (\vartheta + \chi))^i E_1 \left(\frac{t}{\lambda_k} \right) dt \\ = \sum_{i=1}^{m_f-1} \frac{1}{i!} \left(\frac{m_f}{\omega \lambda_f} \right)^i \left\{ (-1)^i (\vartheta + \chi)^i \int_{\vartheta + \chi}^{\infty} \exp \left(-x \left(\frac{1}{\lambda_h} + \frac{m_f}{\omega \lambda_f} \right) \right) E_1 \left(\frac{t}{\lambda_k} \right) dx \right. \\ \left. + \sum_{k=1}^i \binom{i}{k} (-\vartheta + \chi)^{i-k} \int_{\vartheta + \chi}^{\infty} t^k \exp \left(-x \left(\frac{1}{\lambda_h} + \frac{m_f}{\omega \lambda_f} \right) \right) E_1 \left(\frac{t}{\lambda_k} \right) dx \right\}, \tag{52}$$

and

$$\tau_{431} \triangleq \int_{\vartheta + \chi}^{\infty} \exp \left(-x \left(\frac{1}{\lambda_h} + \frac{m_f}{\omega \lambda_f} \right) \right) E_1 \left(\frac{t}{\lambda_k} \right) dx \\ = \frac{\omega \lambda_f \lambda_h}{\omega \lambda_f + m_f \lambda_h} \left\{ \exp \left(-\left(\frac{1}{\lambda_h} + \frac{m_f}{\omega \lambda_f} \right) (\vartheta + \chi) \right) \right. \\ \left. \times E_1 \left(\frac{\vartheta + \chi}{\lambda_k} \right) - E_1 \left((\vartheta + \chi) \left(\frac{1}{\lambda_k} + \frac{1}{\lambda_h} + \frac{m_f}{\omega \lambda_f} \right) \right) \right\}, \tag{53}$$

where the last integral can be derived by applying (Eq. 3.352.2) given in [35] To this end, pulling everything together and after some simple mathematical manipulations, Theorem 4 is derived. This is the end of the proof.

Funding

The author declares that there is no fund of this work.

Authors' contributions

The individual contributions of each authors to the manuscript are the same. Both authors read and approved the final manuscript.

Competing interests

The author declares that there is no competing interests.

Publisher's Note

Springer Nature remains neutral with regard to jurisdictional claims in published maps and institutional affiliations.

Received: 20 January 2017 Accepted: 23 August 2017

Published online: 07 September 2017

References

1. H Chingoska, Z Hadzi-Velkov, I Nikoloska, N Zlatanov, Resource Allocation in Wireless Powered Communication Networks With Non-Orthogonal Multiple Access. *IEEE Wirel. Commun. Lett.* **5**(6), 684–687 (2016)
2. D-T Do, Energy-Aware Two-Way Relaying Networks under Imperfect Hardware: Optimal Throughput Design and Analysis. *Telecommun. Syst.* (Springer). **62**(2), 449–459 (2015)
3. LR Varshney, in *Proc. of IEEE International Symposium in Information Theory*. Transporting information and energy simultaneously, (Toronto, 2008), pp. 1612–1616

4. X Zhou, R Zhang, CK Ho, Wireless information and power transfer: Architecture design and rate-energy trade-off. *IEEE Trans. Wirel. Commun.* **61**(11), 4754–4767 (2013)
5. AA Nasir, X Zhou, S Durrani, RA Kennedy, Relaying protocols for wireless energy harvesting and information processing. *IEEE Trans. Wirel. Commun.* **12**(7), 3622–3636 (2013)
6. R Zhang, CK Ho, MIMO broadcasting for simultaneous wireless information and power transfer. *IEEE Trans. Wirel. Commun.* **12**(5), 1989–2001 (2013)
7. X Chen, C Yuen, Z Zhang, Wireless energy and information transfer tradeoff for limited feedback multi-antenna systems with energy beamforming. *IEEE Trans. Veh. Technol.* **63**(1), 407–412 (2014)
8. KT Nguyen, DT Do, XX Nguyen, NT Nguyen, DH Ha, in *Proc. of AETA 2015: Recent Advances in Electrical Engineering and Related Sciences*. Wireless information and power transfer for full duplex relaying networks: performance analysis, (Ho Chi Minh, 2015), pp. 53–62
9. HS Nguyen, DT Do, M Voznak, Two-Way Relaying Networks in Green Communications for 5G: Optimal Throughput and Trade-off between Relay Distance on Power Splitting-based and Time Switching-based Relaying SWIPT. *AEU Int. J. Electron. Commun.* **70**(3), 1637–1644 (2016)
10. DT Do, HS Nguyen, A Tractable Approach to Analyze the Energy-Aware Two-way Relaying Networks in Presence of Co-channel Interference. *EURASIP J. Wirel. Commun. Netw.* **271** (2016)
11. DWK Ng, ES Lo, R Schober, Wireless information and power transfer: energy efficiency optimization in OFDMA systems. *IEEE Trans. Wirel. Commun.* **12**(12), 6352–6370 (2013)
12. X Chen, C Yuen, Z Zhang, Wireless energy and information transfer tradeoff for limited feedback multi-antenna systems with energy beamforming. *IEEE Trans. Veh. Technol.* **63**(1), 407–412 (2014)
13. G Yang, CK Ho, YL Guan, Dynamic resource allocation for multiple-antenna wireless power transfer. *IEEE Trans. Signal Process.* **62**(14), 3565–3577 (2014)
14. DS Michalopoulos, HA Suraweera, R Schober, Relay selection for simultaneous information transmission and wireless energy transfer: A tradeoff perspective. *IEEE J. Sel. Areas Commun.* **33**(8), 1578–1594 (2015)
15. Z Ding, I Krikidis, B Sharif, HV Poor, Wireless information and power transfer in cooperative networks with spatially random relays. *IEEE Trans. Wirel. Commun.* **13**(8), 4440–4453 (2014)
16. I Krikidis, Relay selection in wireless powered cooperative networks with energy storage. *IEEE J. Sel. Areas Commun.* **33**(12), 2596–2610 (2015)
17. L Chen, S Han, W Meng, C Li, Optimal Power Allocation for Dual-Hop Full-Duplex Decode-and-Forward Relay. *IEEE Commun. Lett.* **19**(3), 471–474 (2015)
18. M Duarte, C Dick, A Sabharwal, Experiment-driven characterization of full-duplex wireless systems. *IEEE Trans. Wirel. Commun.* **11**(12), 4296–4307 (2012)
19. Y Hua, P Liang, Y Ma, AC Cirik, Q Gao, A method for broadband full-duplex MIMO radio. *IEEE Signal Process. Lett.* **19**(12), 793–796 (2012)
20. H Liu, KJ Kim, KS Kwak, HV Poor, Power Splitting-Based SWIPT With Decode-and-Forward Full-Duplex Relaying. *IEEE Trans. Wirel. Commun.* **15**(11), 7561–7577 (2016)
21. I Krikidis, HA Suraweera, PJ Smith, C Yuen, Full-duplex relay selection for amplify-and-forward cooperative networks. *IEEE Trans. Wirel. Commun.* **11**(12), 4381–4393 (2012)
22. K Tutuncuoglu, A Yener, Optimum transmission policies for battery limited energy harvesting nodes. *IEEE Trans. Wirel. Commun.* **11**(3), 1180–1189 (2012)
23. J Yang, S Ulukus, Optimal packet scheduling in an energy harvesting communication system. *IEEE Trans. Commun.* **60**(1), 220–230 (2012)
24. F Yuan, Q Zhang, S Jin, H Zhu, Optimal harvest-use-store strategy for energy harvesting wireless systems. *IEEE Trans. Wirel. Commun.* **14**(2), 698–710 (2015)
25. J Xu, R Zhang, Throughput optimal policies for energy harvesting wireless transmitters with non-ideal circuit power. *IEEE J. Select. Areas Commun.* **32**(2), 322–332 (2014)
26. Z Chen, Y Dong, P Fan, KB Letaief, Optimal Throughput for Two-Way Relaying: Energy Harvesting and Energy Co-Operation. *IEEE J. Sel. Areas Commun.* **34**(5), 1448–1462 (2016)
27. C Zhong, HA Suraweera, G Zheng, I Krikidis, Z Zhang, Wireless information and power transfer with full duplex relaying. *IEEE Trans. Commun.* **62**(10), 3447–3461 (2014)
28. Y Zeng, R Zhang, Full-duplex wireless-powered relay with self-energy recycling. *IEEE Wirel. Commun. Lett.* **4**(2), 201–204 (2015)
29. M Mohammadi, BK Chalise, HA Suraweera, C Zhong, G Zheng, I Krikidis, Throughput analysis and optimization of wireless-powered multiple antenna full-duplex relay systems. *IEEE Trans. Commun.* **64**(4), 1769–1785 (2016)
30. Z Ding, C Zhong, DWK Ng, M Peng, HA Suraweera, R Schober, HV Poor, Application of smart antenna technologies in simultaneous wireless information and power transfer. *IEEE Commun. Mag.* **53**(4), 86–93 (2015)
31. X Ji, J Xu, YL Che, Z Fei, R Zhang, Adaptive Mode Switching for Cognitive Wireless Powered Communication Systems. *IEEE Wirel. Commun. Letters.* **6**(3), 386–389 (2017)
32. H Ding, X Wang, DB da Costa, Y Chen, F Gong, Adaptive Time-Switching Based Energy Harvesting Relaying Protocols. *IEEE Trans. Commun.* **65**(7), 2821–2837 (2017)
33. AA Nasir, X Zhou, S Durrani, RA Kennedy, Wireless-powered relays in cooperative communications: Time-switching relaying protocols and throughput analysis. *IEEE Trans. Commun.* **63**(5), 1607–1622 (2015)
34. RM Corless, GH Gonnet, DE Hare, DJ Jeffrey, DE Knuth, On the Lambert W function. *Adv. Comput. Math.* **5**(1), 329–359 (1996)
35. A Jeffrey, D Zwillinger, *Table of integrals, series, and products*, 7th edn. (Academic Press, New York, 2007)

Submit your manuscript to a SpringerOpen® journal and benefit from:

- Convenient online submission
- Rigorous peer review
- Open access: articles freely available online
- High visibility within the field
- Retaining the copyright to your article

Submit your next manuscript at ► springeropen.com